

Collective roughening of elastic lines with hard core interaction in a disordered environment

Viljo Petäjä¹, Deok-Sun Lee², Mikko Alava^{1,3} and Heiko Rieger²

¹ Helsinki University of Technology, Laboratory of Physics, PO Box 1100, 02015 HUT, Finland

² Theoretische Physik, Universität des Saarlandes, 66041 Saarbrücken, Germany
E-mail: vip@fyslab.hut.fi, dslee@lusi.uni-sb.de, mja@fyslab.hut.fi and physhr@rz.uni-saarland.de

Received 2 July 2004

Accepted 15 October 2004

Published 27 October 2004

Online at stacks.iop.org/JSTAT/2004/P10010

doi:10.1088/1742-5468/2004/10/P10010

Abstract. We investigate by exact optimization methods the roughening of two- and three-dimensional systems of elastic lines with point disorder and hard core repulsion with open boundary conditions. In two dimensions we find logarithmic behaviour whereas in three dimensions we find simple random walk-like behaviour. The line ‘forests’ become asymptotically completely *entangled* as the system height is increased at fixed line density due to increasing line wandering.

Keywords: disordered systems (theory), vortex matter (theory)

³ Author to whom any correspondence should be addressed.

Contents

1. Introduction	2
2. Model	3
3. Roughening in 2D	5
4. Roughening in 3D	6
5. Weak and anisotropic disorder distribution	11
6. Conclusions	15
Acknowledgments	16
References	16

1. Introduction

The paradigmatic model for the mixed or Shubnikov phase of a superconductor in a magnetic field is a system of interacting elastic lines, representing the magnetic vortex lines threading the superconductor along the field direction [1]. The number of lines per unit area perpendicular to the field axis, also called the line density ρ , is given by the magnetic field strength and also defines the typical line-to-line distance. The interaction between the lines is repulsive and long ranged but exponentially cut off beyond a screening length, λ . As long as this screening length is larger than the typical line distance $a = 1/\rho^{1/d}$ (i.e. $\lambda > a$) at low temperatures the lines arrange in a periodic pattern, the Abrikosov flux line lattice. In the presence of quenched disorder such as is produced by crystal lattice defects or impurities this long range order is lost and for weak disorder or low magnetic field strengths transformed into quasi-long range order, the Bragg glass phase [2]. For strong disorder the arrangement of lines is highly irregular and the system is in a state that is called the vortex glass [3].

In this paper we want to study the case when the screening length λ is much *smaller* than the typical line distance ($\lambda \ll a$). This corresponds to high magnetic field or strong disorder and small values of λ . From a theoretical point this limiting case is particularly interesting since it corresponds to a situation in which the system cannot be described by an elastic theory, which is based on the assumption of weak disorder and low line density, any more. Perturbative approaches that start from a ground state with long range order and assume small fluctuations turn out to be inappropriate in this strongly disordered situation and one has to rely on numerical calculations to study the low temperature properties.

Here we study the extreme limit of a system of lines in a disordered environment with hard core repulsion. Although our system is inspired by strongly disordered superconductors in a magnetic field it describes the more general situation of a dense system of one-dimensional (line-like) objects that compete for the energetically most favourite locations in the matrix that they live in but repel each other via a hard core exclusion principle—for instance long polymers stretching from one side of a very

inhomogeneous sample to the opposite side. We use a simplified (directed) polymer model and study the disorder averaged ground state properties of this system. To calculate the exact ground states we use an optimization algorithm, the minimum-cost-flow algorithm, which determines the exact optimal solution in polynomial time [11].

We focus on the roughness properties of the lines (i.e. the typical transverse fluctuations of the lines on their way from the top to the bottom of the system) and will show that in two dimensions the steric repulsion between the lines is sufficient to produce the same scaling behaviour of the roughness as predicted by the elastic theories for long range interactions, weak disorder and low line densities. In particular in 2D the hard core repulsion leads to collective rearrangements of the lines that yield a roughness that increases logarithmically with system size, also called super-rough behaviour [6, 7]. In three space dimensions the situation is totally different: elastic theories predict that the roughness increases with the square root of the logarithm of the system size [8], whereas we find for the case that we consider that the lines become more or less transparent to each other and can wander transversely from one side of the sample to the other. Steric repulsion alone is thus not sufficient to restrict the transverse fluctuations of a line system in 3D.

The paper is organized as follows. In the next section we will introduce the model and specify the methods by which we compute and analyse its ground states. In sections 3 and 4 we will present our results for the roughness of the 2D and 3D systems, respectively, and present the corresponding finite size scaling forms. In section 5 we consider various generalization of the disorder, in particular weak and anisotropic randomness, and derive the scaling laws that govern the behaviour of the crossover to the universal scaling forms reported in the previous sections. Section 6 contains a discussion and an outlook.

2. Model

We consider the following model of a system of interacting lines in a two- or three-dimensional disordered environment: the lines live on the bonds of a simple cubic lattice with a lateral width L and a longitudinal height H (i.e. $M = L \times H$ or $M = L \times L \times H$ lattices sites in 2D or 3D, respectively) with free boundary conditions in all directions. The lines start at the bottom plane and end at the top plane; if necessary the entrance and exit points can be fixed. The number N of lines threading the sample is fixed by a prescribed density $\rho = N/L$ and $\rho = N/L^2$ in two and three dimensions respectively. We restrict ourselves to hard core interactions between the lines, which means that their configuration is specified by bond variables $n_i \in \{0, 1\}$, $n_i = 1$ indicating that a line segment occupies a bond with index i and $n_i = 0$ indicating that no line segment occupies this bond.

We model the disordered environment by assigning a random (potential) energy $e_i \in [0, 1]$ (uniformly distributed) to each bond i , such that the total energy of the line configuration is given by

$$\mathcal{H} = \sum_i e_i n_i. \quad (1)$$

In section 5 the distribution of e_i is modified from that presented above in order to extend our analysis also to the cases of weak and anisotropic disorder.

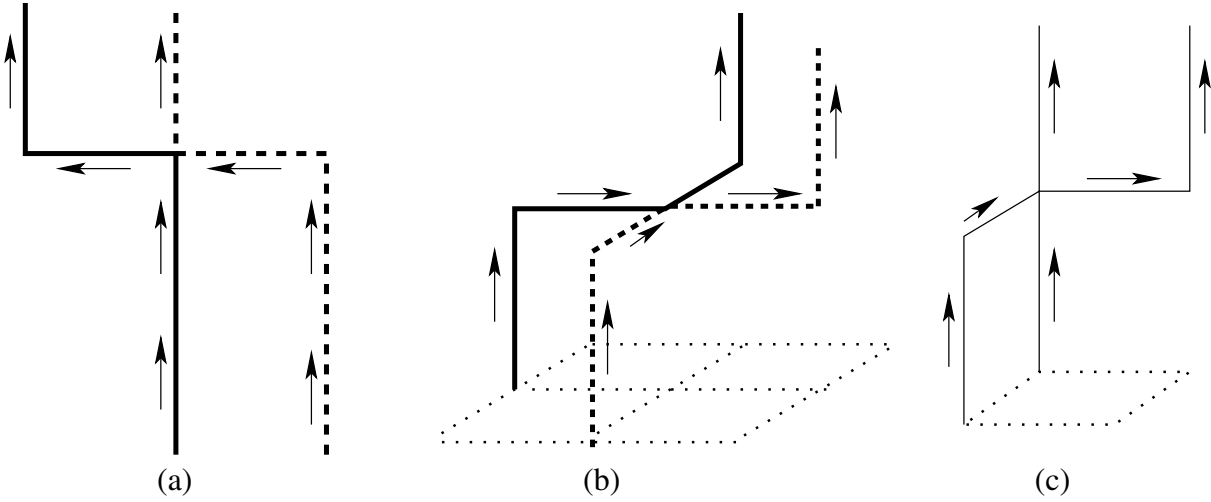


Figure 1. Line identification schemes in two and three dimensions. In (a) and (b) the bold and dotted lines denote the choice of identification of two lines. (c) An example of the case where lines are identified randomly.

In a continuum limit the system of interacting elastic lines is described by the following Hamiltonian:

$$\mathcal{H} = \sum_{i=1}^N \int_0^H dz \left\{ \frac{\gamma}{2} \left[\frac{d\mathbf{r}_i}{dz} \right]^2 + V_r[\mathbf{r}_i(z), z] + \sum_{j(\neq i)} V_{\text{int}}[\mathbf{r}_i(z) - \mathbf{r}_j(z)] \right\}, \quad (2)$$

where $\mathbf{r}_i(z)$ denotes the transverse coordinate at longitudinal height z of the i th flux line. Our numerical model corresponds to the case where the interactions $V_{\text{int}}[\mathbf{r}_i(z) - \mathbf{r}_j(z)]$ are hard core repulsive and the δ -correlated disorder potential $V_r[\mathbf{r}_i(z), z]$ has to be strong compared to the elastic energy which is proportional to γ .

At low temperature the line configurations will be dominated by the disorder and thermal fluctuations are negligible. Therefore we restrict ourselves to zero temperature and focus on the ground state of the Hamiltonian (1). Computing the ground state now corresponds to finding N non-overlapping paths traversing the network from top to bottom. One has to minimize the total energy of the whole set of the paths and not of each path individually (already the two-line problem is actually non-separable [10]). This task can be achieved by applying Dijkstra's shortest path algorithm successively on a residual graph [11].

Although the lines cannot occupy the same bond of the lattice they may touch at isolated points as exemplified in figure 1. This means that the line identification based upon a bond configuration is not unique. Since we want to calculate the roughness of lines we need to determine the individual lines, for which we use a local rule. In 2D the line identification is unambiguous if we simply require that the lines cannot cross; see figure 1(a). The same rule is applied in 3D when the line segments ending in a single site are within the same plane (see figure 1(b)); otherwise the choice is random (see figure 1(c)).

3. Roughening in 2D

The main quantity that we are interested in is the disorder averaged line roughness. The mean square displacement of a single line with index i in one sample is defined as

$$w_i^2 = \overline{r^2}_i - \overline{r}_i^2 \quad (3)$$

with $\overline{r^n}_i = H^{-1} \sum_{z=1}^H r_i^n(z)$ for $n = 1, 2$. The mean square displacement of all lines in one sample is $\overline{w^2} = (1/N) \sum_{i=1}^N w_i^2$ and the roughness w is defined as the square root of the disorder averaged sample mean square displacement $w = \sqrt{\langle \overline{w^2} \rangle}$.

The roughness of a one line system ($N = 1$) scales as $w \sim H^\zeta$ in the limit of infinite transverse system size. In 2D the value of the roughness exponent is $\zeta = 2/3$ [4], whereas in 3D it is close to $\zeta = 5/8$ [5, 12]. In the case of a non-vanishing line density one expects to observe this single-line behaviour as long as the transverse fluctuations of the individual lines are smaller than the average line-to-line distance a , which is given by the line density $\rho = 1/a$ in 2D. This means that we expect $w \sim H^\zeta$ for $H \ll a^{1/\zeta}$.

Once the transverse fluctuations of the individual lines have reached the size of the average line-to-line distance one expects a collective behaviour of the lines that restricts the individual line roughness due to the presence of the others. If the line system behaves like an elastic medium the roughness in the collective regime is expected to behave like $w \sim \ln L$ [6]. Hence, for fixed line density ρ we expect the following scaling form:

$$w \approx a \ln(L) \cdot g_{2D}(H/(a \ln L)^{1/\zeta}), \quad (4)$$

where $g_{2D}(x)$ is a scaling function with the asymptotic behaviour $g_{2D}(x) \propto x^\zeta$ for $x \ll 1$, corresponding to the single-line behaviour, and $g_{2D}(x) = \text{constant}$ for $x \gg 1$, corresponding to the collective regime. Note that we have assumed that the line density enters this form only via a rescaling of the lateral length scales.

We computed the ground states of a large number of disorder realizations (up to 10^3) for various values of L , H and ρ and produced scaling plots for fixed line density ρ according to the suggested size scaling form (4). We found a good data collapse for all values of ρ that we checked ($\rho = 0.05, \dots, 0.5$). In figure 2 we show the data collapse for $\rho = 0.05$. This particular value results in the best data collapse for the achievable system sizes.

We estimated the saturation roughness $w_{\text{sat}} = \lim_{H \rightarrow \infty} w(H)$ from the flat tail of the roughness curves $w(H)$ and show them in figure 3 as a function of L for several values of the line density ρ . The data can be fitted to the form $y = A + B \ln(L)$ again reflecting the collective super-rough scaling of the roughness in 2D. The slope B of the data sets decreases as ρ increases while the constant part A does not vary much. This leads to the strengthening of finite size effects with increasing ρ .

The crossover from single-line to multi-line scaling takes place when $H^\zeta \sim a$, where a is the average line-to-line distance $a = 1/\rho$ in 2D. For fixed but large lateral system size L the scaling form (4) predicts

$$w \approx a \cdot \tilde{g}_{2D}(H/a^{1/\zeta}) \quad (5)$$

where the scaling function $\tilde{g}_{2D}(x)$ has the asymptotic behaviour $\tilde{g}_{2D}(x) \sim x^\zeta$ for $x \ll 1$ and $\tilde{g}_{2D}(x) \sim \text{constant}$ for $x \gg 1$. Figure 4 shows the corresponding data collapse of the roughness data that we computed. Note that the height has also been rescaled with a factor of $1 - 1/a$ to account for the limit $\rho \rightarrow 1$.

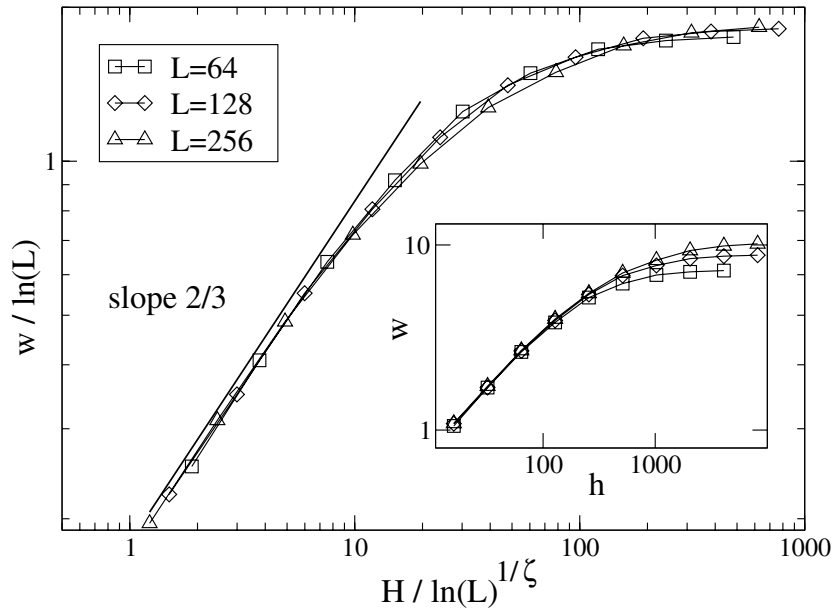


Figure 2. A scaling plot of the roughness in 2D according to the finite size scaling form (4). The line density is $\rho = 0.05$; the roughness exponent is $\zeta = 2/3$.

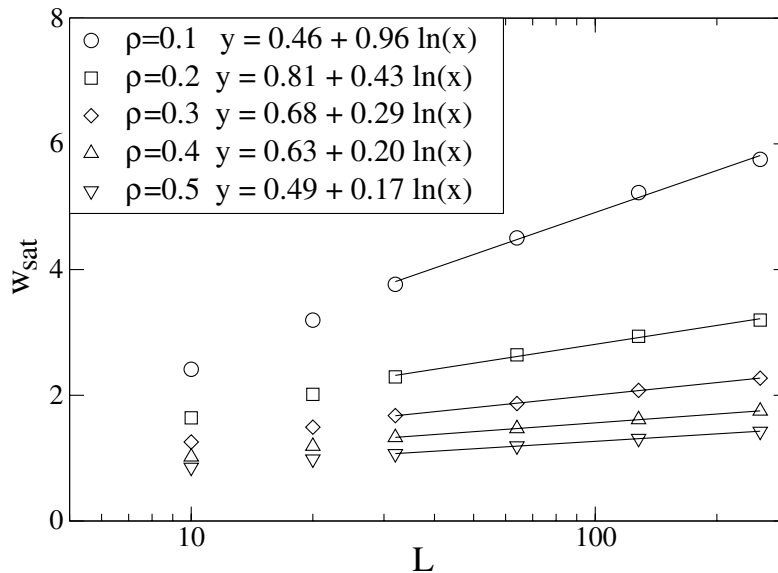


Figure 3. Saturation roughness as a function of the system width with fits of the form $y = A + B \ln(L)$.

4. Roughening in 3D

In this section we present our numerical results and the corresponding scaling laws obtained for the 3D case. If the observations that we made in the last section could be carried over to the 3D case, one would expect two regimes: one for small heights H , in which the transverse fluctuations of the lines are still much smaller than the average

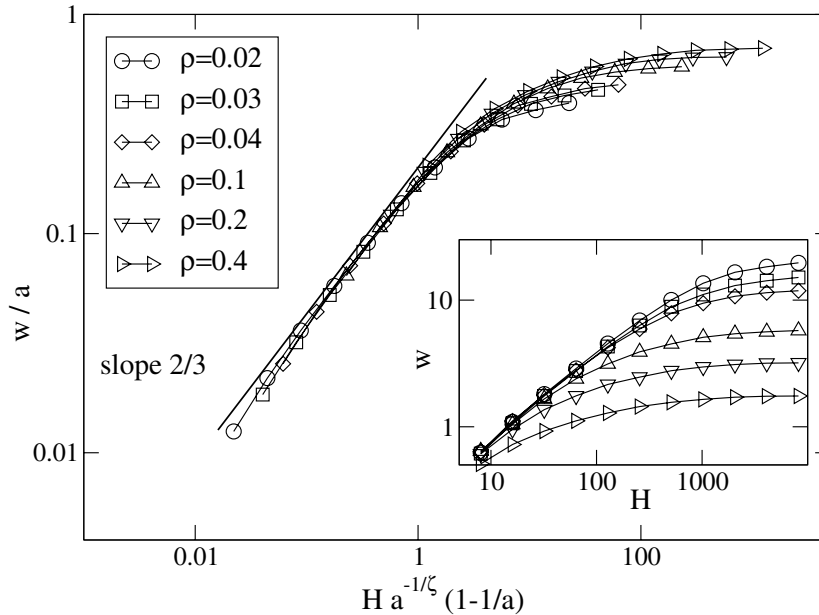


Figure 4. A scaling plot for the roughness in 2D according to the scaling form (5). The system size is fixed at $L = 256$.

line-to-line distance $a = 1/\rho^{1/2}$ in 3D; and one for large H , in which the line roughness is restricted due to collective effects. *Only in the case* where our line system for 3D would also fall into the same universality class as a 3D elastic medium (this is, as we have shown, the case in 2D) would one expect $w_{\text{sat}} \propto \sqrt{\ln L}$ [8, 9].

However, surprisingly, we find (i) three regimes instead of two (see the data shown in figure 5) and (ii) $w_{\text{sat}} \propto L$, i.e. the size of the transverse fluctuations is not restricted by the presence of a large number of other lines but only by the lateral system size. Apparently in 3D the lines become transparent to each other, and the wandering of any line in the transverse direction does not induce collective behaviour.

The three regimes that we find can be characterized as follows:

- (1) A single-line regime for $H \ll a^{1/\zeta}$ in which the roughness behaves as in the one-line case: $w \propto H^\zeta$.
- (2) An intermediate regime for $a^{1/\zeta} \ll H \ll L^2$ in which the roughness increases as $H^{1/2}$, which is identical to the behaviour of random walks. Between the two regimes one can see a crossover that can be shown to be related to the entropic repulsion of the lines. Recall that this leads in 2D asymptotically to collective effects, but here the consequences are different.
- (3) The saturation regime for $H \gg L^2$ in which the roughness saturates at the lateral system size: $w \approx L$.

In the following we support this central result with the data that we obtained from our ground state calculations for the 3D system and derive the appropriate scaling forms for the different regimes.

In figure 6 we show our results for the roughness in 3D in the region of crossover from the intermediate or multi-line regime to the saturation regime. We show data for three

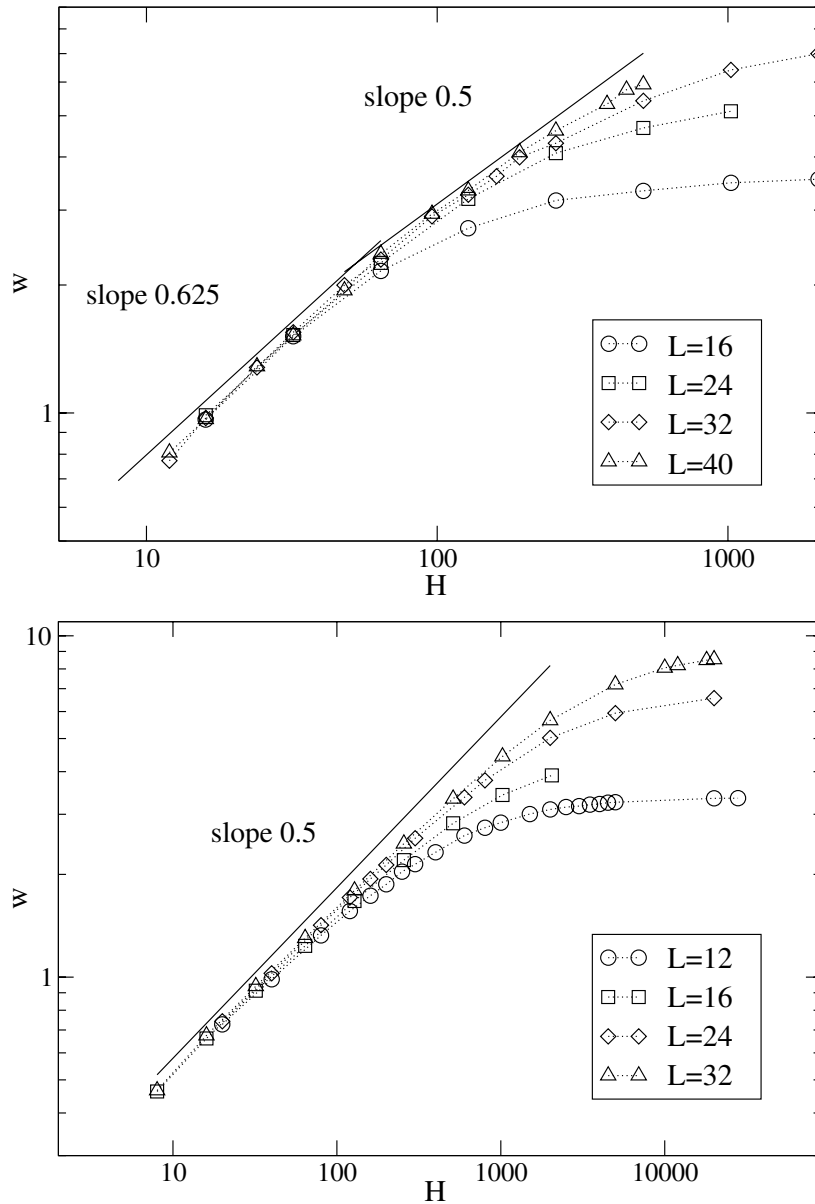


Figure 5. Data for the roughness w as a function of the height H for different transverse system sizes L and two densities: $\rho = 0.005$ (top) and $\rho = 0.4$ (bottom). In the low density limit (top) the crossover from single-line to collective behaviour is visible—indicated by the two straight lines with slope 0.625, the single-line roughness exponent, and 0.5, respectively. In the high density limit the crossover from collective line behaviour (indicated by the straight line with slope 0.5) to the saturation regime is visible. The data points are averaged over 100–1000 samples.

different line density values, but we also have data for other values, and they all fit well into the scenario that we propose now). The finite size scaling plots yield an excellent data collapse using the scaling form

$$w = L \cdot g_{3D}^{(a)}(H/L^2). \quad (6)$$

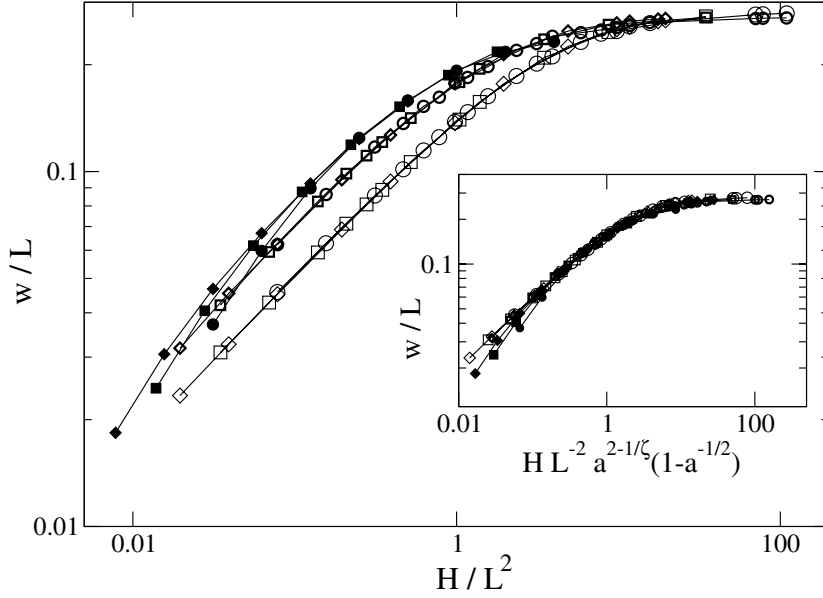


Figure 6. A scaling plot of the roughness in 3D according to the finite size scaling form (6) for different line densities $\rho = 0.1$ (filled symbols), 0.2 (bold) and 0.4 (empty) for system sizes $L = 16$ (ovals), 24 (squares) and 32 (diamonds). The inset shows data collapse according to the scaling form (9).

The scaling function $g_{3D}^{(a)}(x)$, which still depends on a , or the line density $\rho = 1/a^2$, has the following asymptotic behaviour: $g_{3D}^{(a)}(x) \propto x^{1/2}$ for $x \rightarrow 0$ and $g_{3D}^{(a)}(x) = \text{constant}$ for $x \rightarrow \infty$.

The first crucial observation here—and the essential difference from the 2D case—is that in the limit $L \rightarrow \infty$ the roughness is not significantly restricted by the presence of the other lines but approaches a value proportional to the lateral system size. Actually, as we see from the plot of the saturation roughness as a function of L shown in figure 7, $w_{\text{sat}} = \lim_{H \rightarrow \infty} w(L, a) = 0.28 \cdot L + c_a$, where c_a is a small constant that varies only slightly with a . This variation with a is a boundary effect: the free boundary conditions act effectively in a repulsive way on the lines that competes with the steric inter-line repulsion. Therefore systems with a lower line density show smaller transverse line fluctuations than those with a higher density.

The second crucial observation is that the roughness of the lines in the intermediate regime grows like $H^{1/2}$, i.e. they have a roughness exponent that is smaller than the single-line value of $\zeta = 0.625$ and is identical to the value for simple random walks. Although the actual line configuration is constructed in a highly non-trivial manner via a global criterion, namely the computation of the global N -line ground state, their universal geometric properties appear to be similar to that of random walks.

The density dependence of the scaling functions $g_{3D}^{(a)}(x)$ can be worked out by matching it with the scaling form for the single- to multi-line regime. Here the relevant length scale in the H -direction is $a^{1/\zeta}$, and in analogy to the 2D case we expect for $L \gg a$ the L -independent scaling form

$$w = a \cdot \tilde{g}_{3D}(H/a^{1/\zeta}) \quad (7)$$

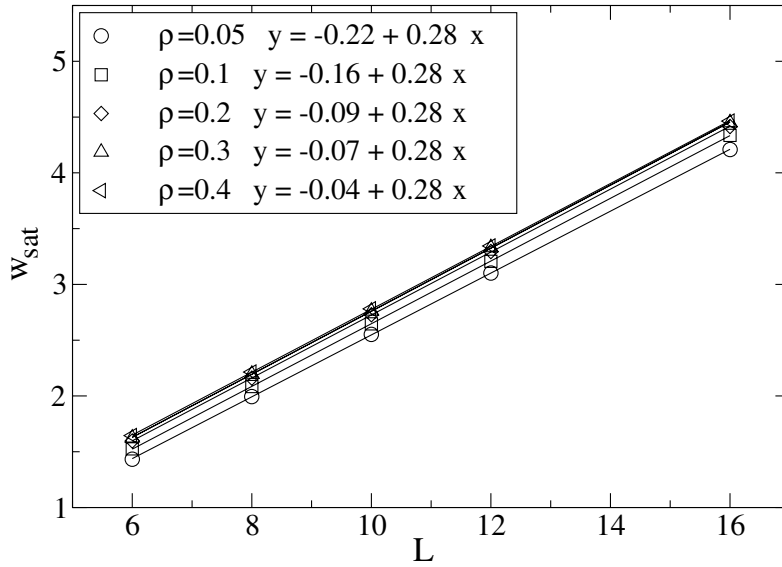


Figure 7. Saturation roughness as a function of the system width with linear fits to the data points.

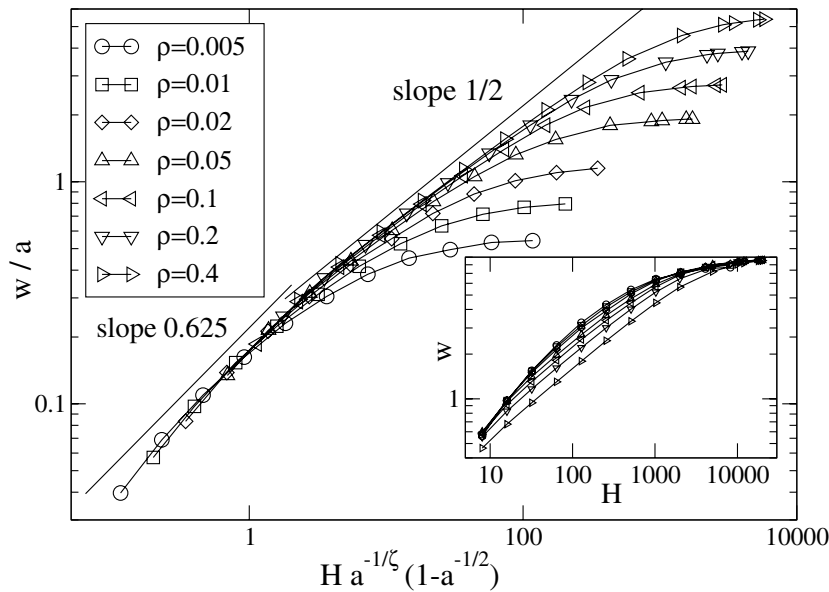


Figure 8. A scaling plot for the roughness in 3D in the crossover region from single- to multi-line behaviour. The system size is $L = 32$. The inset shows the original, unscaled data.

with the asymptotics $\tilde{g}_{3D}(x) = x^\zeta$ for $x \ll 1$ and $\tilde{g}_{3D}(x) = x^{1/2}$ for $x \gg 1$. In figure 8 we show the corresponding scaling plot for the data that we obtained from our calculations. Hence we get the expected single-line behaviour $w \sim H^\zeta$ when $H \ll a^{1/\zeta}$, and we obtain

$$w = a^{1-(1/2\zeta)} H^{1/2} \quad \text{for } w \ll L \quad \text{and} \quad H \gg a^{1/\zeta}. \quad (8)$$

From this the natural scaling variable for the region of crossover from the intermediate regime (where w should be described by (8)) to the saturation regime (where w should be proportional to L according to (6)) appears to be $a^{1-(1/2\zeta)}H^{1/2}/L$ or $H/a^{1/\zeta-2}L^2$, which implies that (6) can be rewritten as

$$w = L \cdot g_{3D}(H/a^{1/\zeta-2}L^2) \quad \text{for } H \gg a^{1/\zeta} \quad (9)$$

with $g_{3D}(x) = x^{1/2}$ for $x \rightarrow 0$ and $g_{3D}(x) = 0.28$ for $x \rightarrow \infty$ (see the inset in figure 6). As in 2D, for high line densities $\rho > 0.1$ ($a \lesssim 3$), one has to take into account the limiting case $\rho = 1$ where lines fill all parallel lattice bonds resulting in zero roughness. This limit can be incorporated into (9) by rescaling H by $1/(1 - \rho)$.

At this point we would like to stress that the random walk-like scaling is *not* related to the actual distance at which the lines touch or cross each other (and are in some cases continued randomly). Both in 2D and in 3D the typical length scale s between two consecutive intersection points on one line is much larger than the length scale ξ for the crossover from single-line to collective behaviour and its divergence with the line average distance a is much stronger. This can be seen in figure 9, where we show scaling plots for the average length of line segments s between two crossings, from which one concludes that s scales with a as $a^{2.6}$ in 2D (compared to $a^{1.5}$ for the crossover length scale ξ) and $a^{3.2}$ in 3D (compared to $a^{1.6}$ for ξ). This also demonstrates that the lines do *not* behave like independent random walkers in 3D but reflect the effect of a steric repulsion that tends to avoid random crossings between them (visible in 2D and in 3D).

The main result of calculations for the 3D system is that the lines with only hard core repulsion can transverse the whole system, in marked contrast to the 2D case. One can visualize this result also by looking at the disorder averaged position of the centre of mass of the individual lines (which is \bar{r} as defined under (3)). In 2D they constitute a regular array on the baseline with lattice spacing a . In 3D, as we show in figure 10, they still constitute a regular array, but it concentrates, with increasing height, more and more in the central region of the basal plane of the system. In the limit $H \rightarrow \infty$ the average centre of mass position of each individual line will be exactly at the centre of the system since nothing restricts it from traversing the system from one side to the other.

5. Weak and anisotropic disorder distribution

Next we check the robustness of the universal scaling forms in equations (4)–(6) against a more general disorder distribution. The random energy e_i is distributed in $[0, \delta]$ with $\delta > 0$ if the bond i is in the transverse direction while it is in $[1 - \epsilon, 1 + \epsilon]$ with $0 \leq \epsilon \leq 1$ if the bond is in the longitudinal direction. The disorder distributions on the transverse bonds and the longitudinal ones are thus different unless $\epsilon = 1$ and $\delta = 2$. Moreover, as ϵ becomes smaller, the energies on the longitudinal bonds are more highly concentrated around 1 implying weaker disorder.

When $\epsilon = 0$ or $\delta^{-1} = 0$, the lines are flat, i.e., $w = 0$ because there is no energy reduction that compensates for the energy cost accompanying a transverse fluctuation. On the other hand, when $\epsilon = 1$ and $\delta = 2$, the lines are rough and exhibit the universal scaling behaviour shown previously. Therefore it would be desirable to find the boundary between two such distinct limits in the (ϵ, δ) plane. We computed the roughness for the generalized disorder distribution with various values of ϵ and δ ; it is shown in figures 11 (2D)

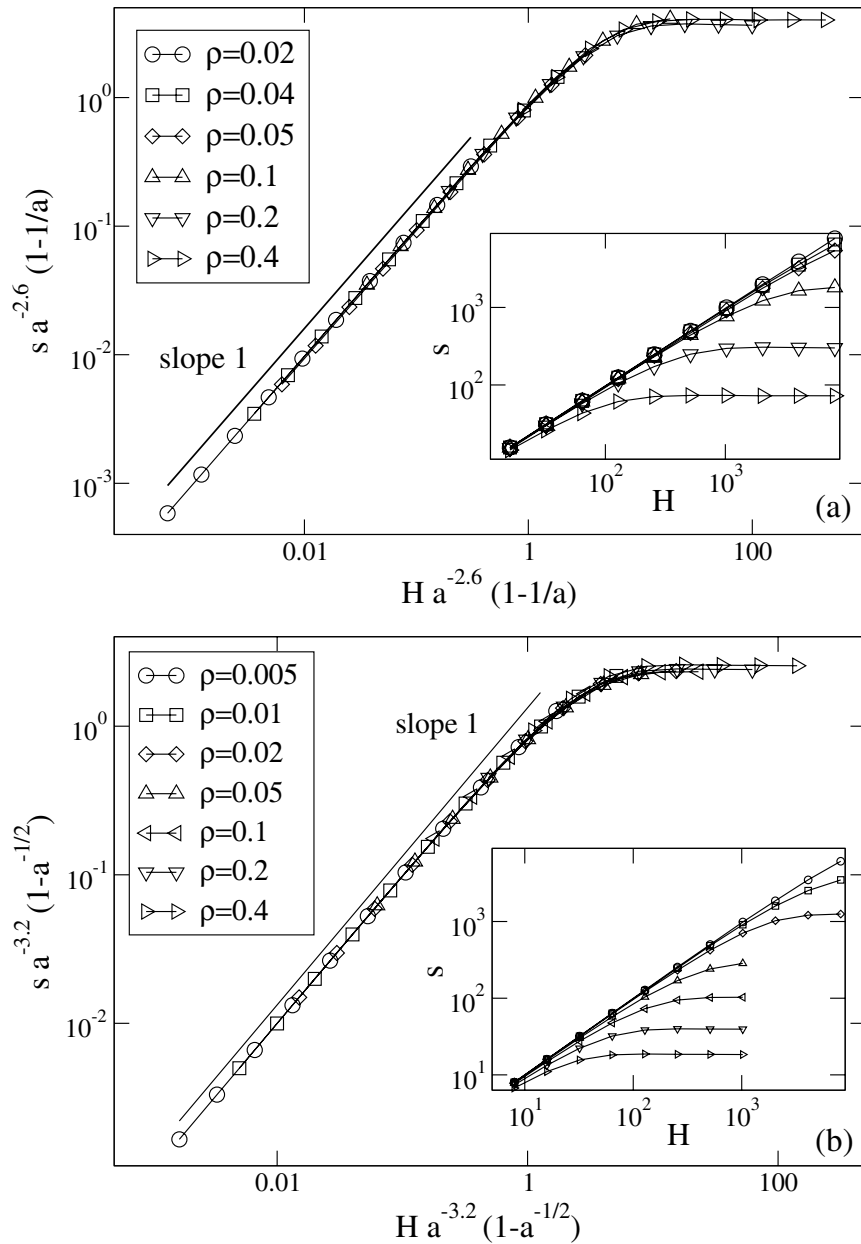


Figure 9. Scaling plots for the lengths of line segments s between two crossings (a) in 2D; the system size is $L = 256$ and (b) in 3D; the system size is $L = 32$. The insets show the original, unscaled data.

and 12 (3D). We consider 2D systems with the fixed line density $N/L = 1/16$. In 3D, a single line is studied to sort out the effect of ϵ and δ on the roughness scaling in equations (4)–(6) more clearly. The roughness shows the same scaling behaviours as in the previous sections except for the dependence on ϵ and δ^{-1} and that the scaling behaviours in equations (4)–(6) are universal with respect to the variations of the disorder distribution used here.

Collective roughening of elastic lines with hard core interaction in a disordered environment

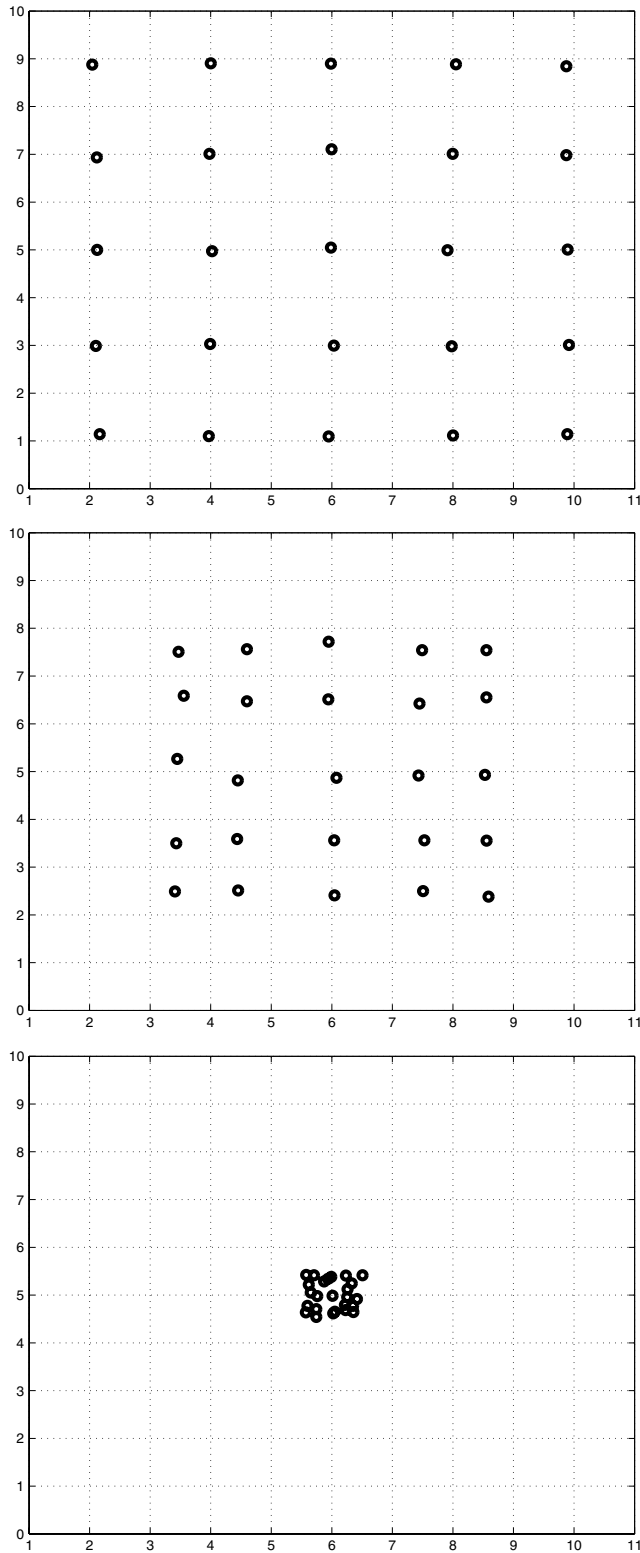


Figure 10. Average positions of centres of mass of lines with fixed starting points. From the top: $H = 10, 100, 1000$. Note that the centre of mass position is averaged over the disorder, here for 1000 samples.

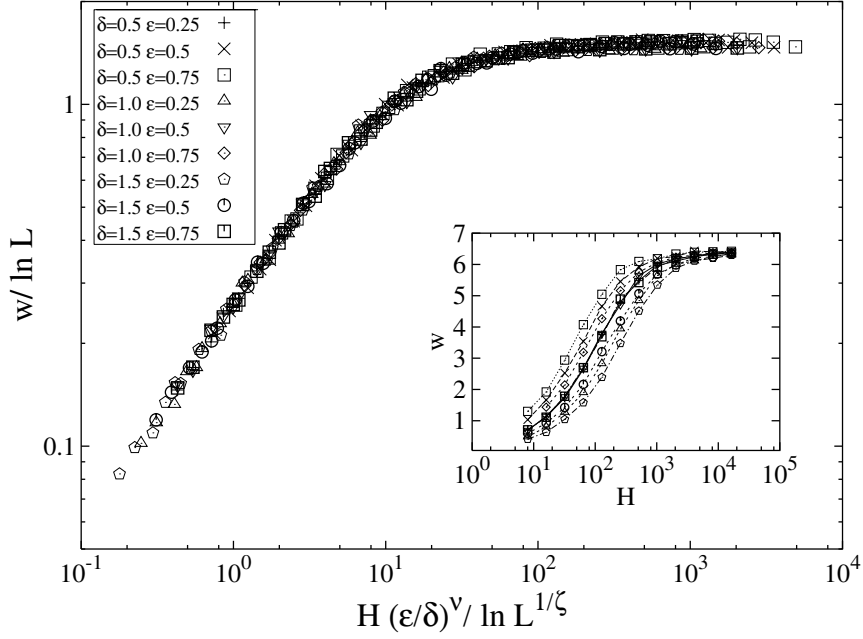


Figure 11. Data collapse of the scaled roughness $w/\ln L$ versus the scaling variable $H(\epsilon/\delta)^\nu/(\ln L)^{1/\zeta}$ of interacting lines in the 2D lattice of size $L \times H$ with $L = 16, 32, 64$ and 128 and the line density $N/L = 1/16$. The parameters ϵ and δ are chosen as in the legend. The exact wandering exponent $\zeta = 2/3$ [12] and the fitting value $\nu \simeq 0.8(1)$ are used for the scaling variable. The inset is the plot of the roughness w versus H for $L = 64$. The dependence of w on ϵ and δ is shown before the roughness saturates.

The dependence of the roughness on ϵ and δ before it saturates is rooted in the crossover behaviour around the point $(\epsilon, \delta^{-1}) = (0, 0)$. As (ϵ, δ^{-1}) deviates from $(0, 0)$, a line roughens ($w > 0$) if the reduction of the longitudinal bond energy obtained by the transverse fluctuation is larger than the accompanying energy cost. By comparing the energy reduction and cost accompanying the transverse fluctuation, one can get the crossover (‘Larkin’) length scale for H , ξ_H . For a given line i , the typical fluctuation or the standard deviation of the sum of the energies on the longitudinal bonds, $E_{i,\parallel} = \sum_z e_{\parallel}(\mathbf{r}_i(z))$, is given by $\epsilon\sqrt{H}$, which corresponds to the average reduction of $E_{i,\parallel}$ achieved by a transverse fluctuation. On the other hand, the line chooses the position, among H possible ones ($1 \leq z \leq H$), where the cost is minimum for fluctuating in the transverse direction. The cost on average is equal to the average minimum value of H independent random variables each of which is distributed uniformly in $[0, \delta]$, which is given by $\delta/(H + 1)$ [13]. Comparing the energy reduction and cost, one finds the characteristic length scale ξ_H as

$$\xi_H \sim \left(\frac{\epsilon}{\delta}\right)^{-2/3}, \quad (10)$$

such that the roughness w is zero for $H \ll \xi_H$ and non-zero, increasing as H^ζ , for $H \gg \xi_H$. From the numerical data and the above argument, the roughness in 2D and 3D for the

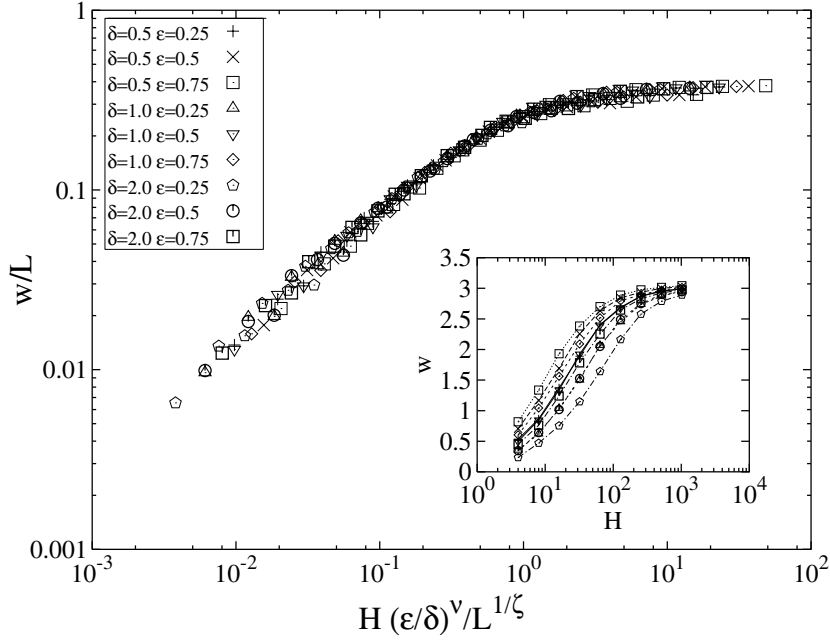


Figure 12. Data collapse of the scaled roughness w/L versus the scaling variable $H(\epsilon/\delta)^\nu/L^{1/\zeta}$ of one line in the 3D lattice of size $L \times L \times H$ with $L = 8, 16$ and 32 . The wandering exponent $\zeta = 0.625$ [12, 14] is used and the exponent ν is found to be $0.68(8)$. The inset is the plot of the roughness w versus H for $L = 8$.

generalized disorder distribution used here can be represented as

$$w \sim \begin{cases} 0 & \left(\frac{H}{\xi_H} \ll 1 \right), \\ \left(\frac{H}{\xi_H} \right)^\zeta & \left(1 \ll \frac{H}{\xi_H} \ll [w_{\text{sat}}(L)]^{1/\zeta} \right), \\ w_{\text{sat}}(L) & \left(\frac{H}{\xi_H} \gg [w_{\text{sat}}(L)]^{1/\zeta} \right), \end{cases} \quad (11)$$

with the usual roughness exponents and saturation roughness scalings according to the dimension. The crossover scaling function between the transient regime and the stationary state is represented in terms of the scaling variable $H/(\xi_H(w_{\text{sat}}(L))^{1/\zeta})$, which is shown in figures 11 and 12 with the fitting value for ν in $\xi_H \sim (\epsilon/\delta)^{-\nu}$ being $0.8(1)$ (two dimensions) and $0.68(8)$ (three dimensions), the latter being in rather good agreement with $2/3$. The derivation of (10) corresponds to comparing elastic energy to the pinning energy in a conventional derivation of the Larkin length. Obviously in two dimensions one should be more careful when simply equating the costs of transverse bonds to the elastic energy of the line and the costs of longitudinal bonds to the strength of a pinning potential.

6. Conclusions

In this work we have considered the collective effects arising from the interaction of ‘forests’ of directed polymers, in the presence of quenched randomness. In both 2D and 3D this is

marked by a crossover from individual, rough lines to a ‘collective’ regime with a system size dependent roughness w . In 2D, our studies augment earlier work on similar systems using fixed line densities. The approach is based on a mapping of the problem to the minimal matching problem of combinatorial optimization, and the essential point of our model(s) is that the density of lines is a free parameter. In this, we consider the crossover to the asymptotic collective roughness as a function of the parallel and perpendicular disorder strengths.

In 3D, perhaps more importantly, it is found that the generally expected logarithmic roughening is absent: while (scalar) models of weakly perturbed elastic manifolds do exhibit logarithmic roughness scaling this is not the case here. An ensemble of directed polymers with hard core interactions exhibits almost ‘trivial’ roughening, with a random walk-like scaling picture. There is a crucial difference between two and three spatial dimensions even within the confines of the same microscopic model. An ensemble of directed polymers with locally repulsive interactions is thus proven to be different from other approaches using mappings to e.g. higher dimensional manifolds that do exhibit logarithmic correlations [9]. It is worth noting that this does not follow from a ‘proliferation of dislocations’ in a vortex lattice, but from the absence of collective behaviour.

A rather random but likewise potentially very important consequence of the same is that in 3D the lines entangle—the topological state becomes highly non-trivial such that it might be useful to describe it in terms of knot theory [15, 16]. Such concomitant geometrical structures are again absent in models for 3D elastic media. In this case, the description of barriers and excitations still remains to be given, including the effect of the entanglement on both.

Acknowledgments

We acknowledge gratefully the support of the European Science foundation (ESF) SPHINX network, the Deutsche Forschungsgemeinschaft (DFG), and (MJA, VIP) the Centre of Excellence programme of the Academy of Finland.

References

- [1] For a review see Blatter G *et al*, 1994 *Rev. Mod. Phys.* **66** 1125
- [2] Nattermann T, 1990 *Phys. Rev. Lett.* **64** 2454
Giarmachi T and Le Doussal P, 1994 *Phys. Rev. Lett.* **72** 1530
Giarmachi T and Le Doussal P, 1995 *Phys. Rev. B* **52** 1242
- [3] Fisher M P A, 1989 *Phys. Rev. Lett.* **62** 1415
Fisher D S *et al*, 1991 *Phys. Rev. B* **43** 130
- [4] Huse D A and Henley C L, 1985 *Phys. Rev. Lett.* **54** 2708
Kardar M, 1985 *Phys. Rev. Lett.* **55** 2924
Huse D A, Henley C L and Fisher D S, 1985 *Phys. Rev. Lett.* **55** 2924
- [5] Forrest B M and Tang L H, 1990 *Phys. Rev. Lett.* **64** 1405
Kim J M, Moore M A and Bray A J, 1991 *Phys. Rev. A* **44** 2345
- [6] Toner J and DiVincenzo D P, 1990 *Phys. Rev. B* **41** 632
Hwa T and Fisher D S, 1994 *Phys. Rev. Lett.* **72** 2466
- [7] Zeng C, Middleton A A and Shapir Y, 1996 *Phys. Rev. Lett.* **77** 3204
Bogner S, Emig T and Nattermann T, 2001 *Phys. Rev. B* **63** 174501
- [8] Giarmachi T and Le Doussal P, 1995 *Phys. Rev. B* **52** 1242
- [9] McNamara D and Middleton A A, 1999 *Phys. Rev. B* **60** 10062

- [10] Petäjä V, Alava M and Rieger H, 2001 *Int. J. Mod. Phys. C* **12** 421
- [11] Alava M, Duxbury P, Moukarzel C and Rieger H, 2000 *Phase Transitions and Critical Phenomena* vol 18, ed C Domb and J L Lebowitz (New York: Academic)
Hartmann A and Rieger H, 2002 *Optimization Algorithms in Physics* (Berlin: Wiley-VCH)
- [12] Barabasi A-L and Stanley H E, 1995 *Fractal Concepts in Surface Growth* (Cambridge: Cambridge University Press)
- [13] Gumbel E J, 1958 *Statistics of Extremes* (New York: Columbia University Press)
- [14] Lässig M, 1998 *Phys. Rev. Lett.* **80** 2366
- [15] Petäjä V, Alava M and Rieger H, 2004 *Europhys. Lett.* **66** 778
- [16] Bikbov R and Nechaev S, 2001 *Phys. Rev. Lett.* **87** 150602
Nechaev S K, 1996 *Statistics of Knots and Entangled Random Walks* (Singapore: World Scientific)